

Article

Characterization of Macromolecular Structure and Molecular Dynamics Optimization of Gas Coal: A Case Study of Hongdunzi Coal

Lin Hong ^{1,2,*}, Xingzhu Che ¹, Dan Zheng ^{1,2} and Dameng Gao ^{1,2}

¹ College of Safety Science and Engineering, Liaoning Technical University, Huludao 125105, China; chexingzhu0401@163.com (X.C.); zhengdan@lntu.edu.cn (D.Z.); gaodameng@lntu.edu.cn (D.G.)

² Key Laboratory of Mine Thermal Power Disaster and Prevention, Liaoning Technical University, Ministry of Education, Huludao 125105, China

* Correspondence: honglyn@163.com

Abstract: To investigate the molecular structure characteristics and chemical reaction mechanisms of gas coal from the Hong II coal mine of the Ningxia Hongdunzi Coal Industry, this study explores its elemental composition, structural features, and methods for constructing and optimizing molecular models. The basic properties of the coal were determined through proximate and elemental analyses. The carbon structure was characterized using ¹³C-NMR nuclear magnetic resonance, the N and S chemical states were analyzed with XPS, and the distribution of hydroxyl, aliphatic hydrocarbons, aromatic rings, and oxygen-containing functional groups was characterized by FT-IR. Based on the analysis results, a molecular structure model of Hongdunzi gas coal was constructed with the molecular formula C₂₀₄H₁₁₇O₁₇NS, and the calculated results of the model showed high consistency with the experimental spectra of ¹³C-NMR. The macromolecular model of gas coal was constructed using the Materials Studio 2020 software, and its structure was optimized through geometric optimization and dynamic simulations. After optimization, the total energy of the model was significantly reduced from 8525.12 kcal·mol⁻¹ to 3966.16 kcal·mol⁻¹, highlighting the enhanced stability of the coal molecular structure. This optimization indicates that torsional energy plays a dominant role in molecular stability, while van der Waals forces and electrostatic interactions were significantly improved during the optimization process.



Academic Editor: Qingbang Meng

Received: 29 December 2024

Revised: 10 January 2025

Accepted: 15 January 2025

Published: 19 January 2025

Citation: Hong, L.; Che, X.; Zheng, D.; Gao, D. Characterization of Macromolecular Structure and Molecular Dynamics Optimization of Gas Coal: A Case Study of Hongdunzi Coal. *Processes* **2025**, *13*, 275. <https://doi.org/10.3390/pr13010275>

Copyright: © 2025 by the authors. Licensee MDPI, Basel, Switzerland. This article is an open access article distributed under the terms and conditions of the Creative Commons Attribution (CC BY) license (<https://creativecommons.org/licenses/by/4.0/>).

Keywords: gas coal; 3D molecular structure; ¹³C NMR; FT-IR; XPS

1. Introduction

Coal and other fossil fuels are important resources for supporting future economic and social development [1,2]. With the continuous development of science and theoretical advancements, researchers have increasingly diversified the methods and approaches for studying coal adsorption and molecular structure while attempting to establish accurate molecular models based on various cutting-edge theories. However, coal differs from other macromolecular organic substances, lacking a unified physical and chemical form, and exhibits diversity in molecular composition and complexity in chemical structure [3]. The macromolecular structure of coal is primarily composed of aromatic structural units, aliphatic chain structures, and heteroatom-containing functional groups (such as N, S, and O), with highly crosslinked heterogeneity and multi-scale complexity. This complexity not only makes the scientific construction of coal molecular models a key focus of research but also raises higher demands for the efficient and clean utilization of coal [4].

During the processing, utilization, and combustion of coal, large amounts of pollutants such as dust, flue gas, and slag are generated. Dust contains solid particles like fly ash and carbon particles, while flue gas includes harmful gases such as SO₂, CO, CO₂, and NO_x, causing severe damage to the natural environment and ecology [5]. The generation of these pollutants is closely related to the bond-breaking mechanisms and locations of elements such as N and S within the molecular structure of coal [6]. Wang [7] suggested that studying the composition and structural characteristics of low-rank coal is key to achieving its clean, efficient, and hierarchical utilization, as well as its rational optimization. These studies indicate that achieving clean and efficient utilization of coal requires first investigating its structure at the molecular level. Therefore, precisely constructing molecular structure models of coal at the microscopic level and uncovering the mechanisms of its pyrolysis and combustion reactions have significant theoretical and practical implications for the efficient and clean utilization of coal.

In recent years, significant progress has been made in the study of coal molecular structures, particularly in the construction of molecular models, thanks to advancements in analytical characterization techniques and computational chemistry. Researchers have continuously improved the accuracy and reliability of coal molecular models by combining various advanced experimental techniques and simulation methods. For example, Sharma [8] employed HRTEM image algorithms to precisely extract the stacked structure information of aromatic condensed rings in coal. Xiang [9] constructed the macromolecular structure model of Yanzhou coal using ¹³C CP/MAS NMR data, revealing the distribution characteristics of aromatic and aliphatic structures in coal. Li Zhuangmei [10] utilized multiple characterization techniques such as XPS, FTIR, and ¹³C-NMR, combined with computer-assisted methods, to successfully construct 2D and 3D molecular models of Ningdong Hongshiwang coal, further quantifying its microscopic molecular structure. Zhang Diankai [11] combined infrared spectroscopy, nuclear magnetic resonance, and X-ray photoelectron spectroscopy to construct the molecular model of Yunnan Mile lignite. In addition, Fan Zhihui [12] studied molecular structure models of coal with different degrees of metamorphism and determined their molecular formulas. Gao [13] applied ReaxFF molecular dynamics simulations to investigate the pyrolysis process of subbituminous coal, exploring the relationship between gases produced in the early stages of pyrolysis and functional groups in the coal structure. These research findings provide strong support for the precise characterization of coal molecular structures. However, due to the complexity and diversity of coal molecular structures, the universality and accuracy of these models still face significant challenges, requiring further exploration and optimization.

This study focuses on gas coal from the Hongdunzi coal mine in Ningxia, using methods such as proximate analysis, elemental analysis, ¹³C NMR, XPS, and FT-IR to systematically characterize the chemical composition and functional group distribution of the coal samples, followed by in-depth theoretical analysis. On this basis, a 2D molecular planar model of the coal sample was constructed, and the accuracy of the model was validated through simulated ¹³C NMR spectra. Additionally, the model was optimized in Materials Studio, significantly reducing molecular energy and enhancing stability, thereby accurately constructing a macromolecular model of gas coal. This study provides important theoretical support and practical guidance for uncovering the pyrolysis and combustion mechanisms of coal and achieving its efficient and clean utilization.

2. Materials and Methods

2.1. Sample Collection and Preparation

This study focused on gas coal from the Hong II coal mine of Ningxia Hongdunzi Coal Industry. Coal samples were collected according to the national standard GB/T 482-

2008 [14], with visibly defective parts removed to retain intact and undamaged samples. The collected coal samples were crushed using a crusher to a particle size of less than 2 mm. The samples were then sieved to obtain 200-mesh (<75 μm) coal powder, which was dried in a constant-temperature oven at 80 °C for 12 h. The analysis results are shown in Table 1.

Table 1. Elemental and Proximate Analysis of Coal.

Proximate Analysis w/%				Elemental Analysis w/%				
M_{ad}	A_{ad}	V_{daf}	FC_{daf}	N_{daf}	C_{daf}	H_{daf}	S_{daf}	O_{daf}
0.2	8.869	31.454	59.477	0.782	85.112	4.015 5	0.727 5	9.363

2.2. Experimental Equipment and Parameter Settings

To comprehensively study the physicochemical properties and molecular structural characteristics of coal, this research employed multiple experimental methods for the systematic characterization and analysis of the coal samples.

- (1) According to the Chinese national standard GB/T212-2008 [15], an HXG5005 industrial analyzer was used to measure the ash, fixed carbon, moisture, and volatile matter content of coal. In accordance with GB/T31391-2015 [16], an ELTRA CS-2000 elemental analyzer was used to test the relative contents of the main elements C, H, O, N, and S in the coal.
- (2) A Tensor 27 infrared spectrometer from Bruker (Bremen, Germany) was used for the tests. A suitable amount of coal sample was mixed with potassium bromide at a 1:200 ratio, thoroughly stirred, and then ground. The mixture was pressed into transparent thin sheets with a thickness of 0.2–0.5 mm using a tablet press. The sheets were dried in an oven at 80 °C for 12 h and then measured using the infrared spectrometer. The spectrometer's measurement range was 4,000,400 cm^{-1} , with a resolution of 4.0 cm^{-1} and 32 scans.
- (3) A Thermo Scientific (Waltham, MA USA) TM Nexsa TM X-ray photoelectron spectrometer was used for analysis, with the vacuum level in the analysis chamber maintained at 8×10^{-10} Pa. An Al $K\alpha$ radiation source with a photon energy of 1486.6 eV and a working voltage of 12.5 kV was used. The signals were accumulated over 10 cycles. The pass energy for the full spectrum was set at 100 eV, the narrow spectrum at 30 eV, and the step size at 0.1 eV. The binding energy of C1s (284.80 eV) was used as the energy standard for charge correction.
- (4) The ^{13}C -NMR technique can obtain information about the carbon atom skeleton of coal without damaging its molecular structure. The experimental instrument used was a Bruker AVANCE III HD 600 MHz solid-state nuclear magnetic resonance spectrometer (Bruker, Ferrand, Switzerland), equipped with an H/X dual-resonance solid probe and a 4 mm ZrO₂ rotor with a rotational speed of 5 kHz. The detection resonance frequency for ^{13}C was 100.625 MHz, with a sampling time of 5.12 μs , a spectral width of 50 kHz, and a cycle delay time of 6.5 μs .

2.3. Construction Method for the Gas Coal Structural Model

Based on elemental analysis data, the mass fractions of carbon, oxygen, nitrogen, and sulfur were determined, and the forms and contents of these elements were analyzed using XPS data. FT-IR was used to characterize the distribution of hydroxyl, aliphatic hydrocarbons, aromatic rings, and oxygen-containing functional groups. The carbon skeleton structure information of the coal was quantitatively and qualitatively described using the ^{13}C -NMR spectra, obtaining the relative contents of the aliphatic and aromatic carbons and allowing for the calculation of the organic carbon parameters representing

the molecular structure of gas coal from the Ningxia Hongdunzi coal mine. A molecular planar model was drawn based on the above characterization data. The chemical shifts of each carbon atom in the model were obtained using the MestReNova-15.0.0-34764 software, which were then imported into the g NMR software. At a given frequency, a simulated ^{13}C NMR spectrum was obtained. The connections of structural units in the model were iteratively adjusted and corrected until the experimental and simulated chemical shifts matched well. The model was dynamically optimized using Materials Studio. The specific steps for model construction are shown in Figure 1.

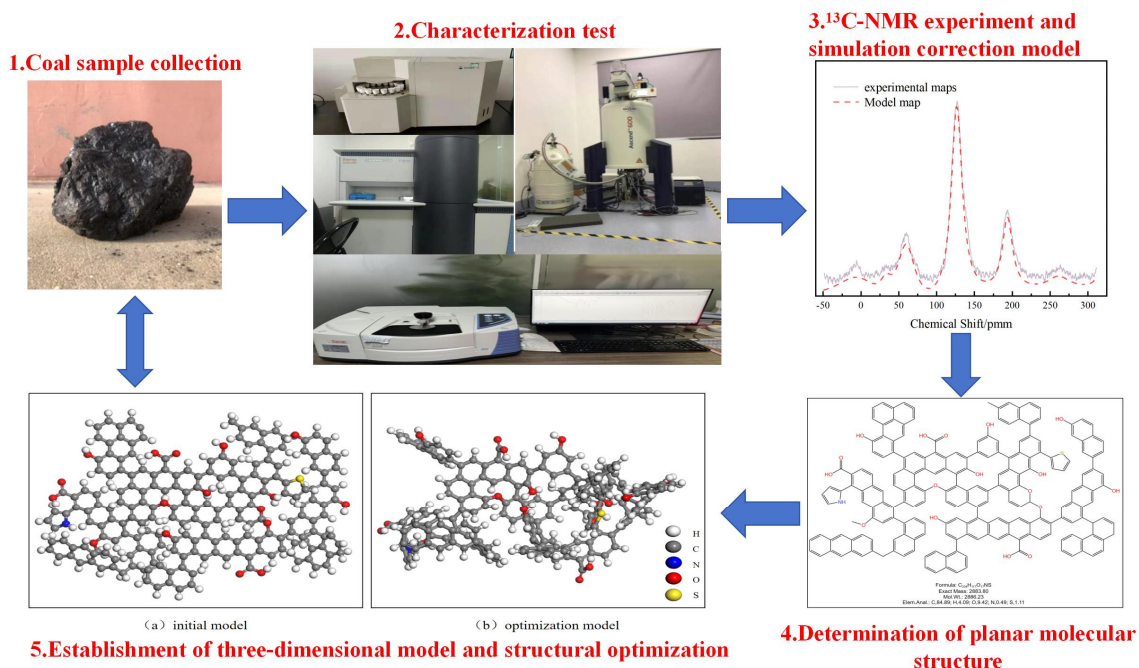


Figure 1. Flow chart for 3D coal macromolecular structure modeling.

3. Results and Analysis

3.1. ^{13}C -NMR

The chemical shift range measured by ^{13}C NMR generally falls between 0 and 250 ppm [17]. The results of the ^{13}C NMR characterization of the coal sample, after peak fitting, are shown in Figure 2, and the categorized chemical shift peaks are summarized in Table 2. The chemical shifts of aliphatic carbons are in the range of 0–80 ppm, with a content of approximately 12.76%. The chemical shifts of aromatic carbons range from 80 to 170 ppm, with a content of approximately 49.32%, while the chemical shifts of carbonyl carbons are located around 200 ppm, with a content of approximately 22.09%. Among the aliphatic carbons, oxygen-bonded aliphatic carbons (corresponding to 58–71 ppm) dominate, accounting for about 9.46%, indicating the presence of abundant oxygen-associated aliphatic carbon structures in the sample, such as carbons in alcohols (C-OH), ethers (C-O-C), or esters (-COO-). Methine and quaternary carbons (corresponding to 43 ppm) are secondary, accounting for about 3.30%, indicating the presence of a small amount of branched or complex aliphatic structures in the sample. However, the overall proportion of aliphatic carbons is low, reflecting a limited amount of hydrophobic components in the sample. Among the aromatic carbons, protonated aromatic carbons (corresponding to 123–127 ppm) dominate, accounting for about 36.40%. The large proportion of protonated aromatic carbons indicates high aromatic structural activity in the sample, such as mono- or sparsely substituted benzene rings, implying that hydrogen in the aromatic system is rarely replaced by other groups. Bridged aromatic carbons (corresponding to 136 ppm)

are secondary, accounting for about 12.92%, and indicate the presence of some condensed aromatic compounds or heterocyclic aromatic compounds, which increases the complexity and aromaticity of the sample. After calculations, the bridgehead carbon to peripheral carbon ratio of gas coal from the Hong II coal mine in Ningxia Hongdunzi Coal Industry is 0.28, indicating a good degree of polycondensation in the aromatic condensed rings.

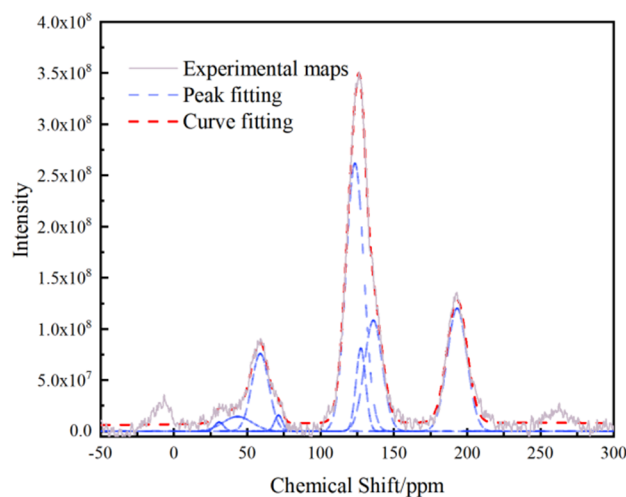


Figure 2. Fitted ^{13}C -NMR Spectrum of Coal Sample.

Table 2. Peak Fitting Parameters of ^{13}C -NMR Spectrum for Coal Sample.

Peak No.	Peak Area	FWHM/ppm	Peak Position/ppm	Peak Area Percentage/%	Functional Group
1	6.91274E7	7.32	30.86	0.53	Methylene, Quaternary Carbon
2	3.5646E8	23.25	43.35	2.77	Methine, Quaternary Carbon
3	1.11264E9	13.77	58.88	8.64	Oxygen-Bonded Aliphatic Carbon
4	1.06628E8	6.44	71.33	0.82	Oxygen-Bonded Aliphatic Carbon
5	6.6625E8	7.72	127.45	5.17	Protonated Aromatic Carbon
6	1.66236E9	14.40	135.99	12.92	Bridged Aromatic Carbon
7	4.01823E9	14.42	123.41	31.23	Protonated Aromatic Carbon
8	2.03278E9	15.90	193.04	15.79	Carboxylic Carbon
9	2.84287E9	666.47	193.04	22.09	Carboxylic Carbon

3.2. XPS

The kinetic energy and quantity of the photoelectrons on the coal sample surface were measured using XPS, yielding the electron binding energies and signal intensities of different elements. These results were then used to infer the elemental composition and relative content of the coal sample [18]. The peak-fitting XPS spectra of sulfur and nitrogen elements are shown in Figure 3, while the forms and contents of N/S elements are presented in Table 3.

Table 3. Forms and Contents of N/S Elements in the Coal Sample.

Element	Peak Number	Peak Position/eV	Peak Area	Relative Area/%	Form
N	1	398.04	1940.76	19.99	Pyridine
	2	399.74	6356.56	65.54	Pyrrrole
	3	402.60	474	4.90	Quaternary Nitrogen
	4	405.19	925.65	9.58	Nitrogen Oxides
S	1	163.30	974.87	27.60	Thiols, Sulfides
	2	164.60	476.41	14.92	Thiophenic Sulfur
	3	168.41	1610.86	50.55	Sulfoxides
	4	172.47	128.33	4.04	Inorganic Sulfur

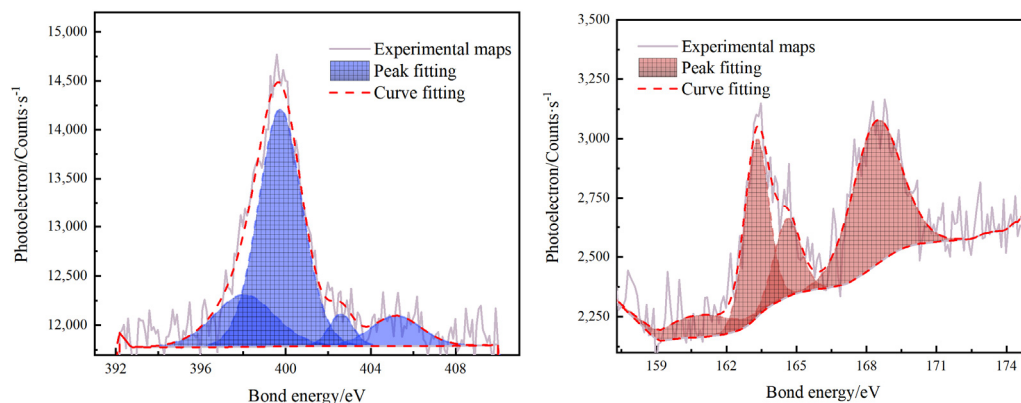


Figure 3. Peak Fitting Spectrum of N/S Elements in the Coal Sample.

The N 1s peak occurs between 399 and 401 eV and is divided into the following four peaks after peak fitting: Pyridinic nitrogen (corresponding to 398 eV) accounts for 19.99% of the N structure. This type of nitrogen forms covalent bonds with carbon in pyridine rings and is typically associated with organic groups in the coal sample, particularly aromatic compounds or nitrogen-containing heterocyclic compounds. Pyrrolic nitrogen (corresponding to 399 eV) accounts for 65.54% of the N structure, indicating that the main form of nitrogen in the coal sample is pyrrolic nitrogen. This suggests a significant presence of nitrogen-containing organic compounds, such as pyrrole structures or similar aromatic nitrogen compounds. Quaternary nitrogen (corresponding to 402 eV) accounts for 4.90% of the N structure. The content of quaternary nitrogen in coal samples is typically low, and this form of nitrogen is generally stable, making it less likely to participate in many reactions. Nitrogen oxides (corresponding to 405 eV) account for 9.58% of the N structure, indicating the presence of a certain proportion of oxidized nitrogen, which likely originates from coal oxidation or gasification processes.

The S 2p peak occurs between 160 and 170 eV and is divided into the following four peaks after peak fitting: Thiols and sulfides (corresponding to 163 eV) account for 27.60% of the S structure. Sulfur in these structures typically exists in a divalent form and is bonded to carbon or hydrogen atoms via single bonds. Thiophene (corresponding to 164 eV) accounts for 14.92% of the S structure. Thiophene sulfur belongs to the aromatic organic sulfur category in coal, and these compounds are relatively stable and occupy a certain proportion of coal's organic fraction. Sulfoxides (corresponding to 168 eV) account for 50.55% of the S structure, indicating that the coal sample underwent oxidation processes, leading to the formation of a large amount of sulfoxide sulfur. Inorganic sulfur (corresponding to 172 eV) accounts for 4.04% of the S structure, indicating the presence of sulfur compounds in the coal sample that are combined with metal ions, such as sulfates (SO_4^{2-}) and hydrogen sulfide (H_2S). The sulfur in the coal sample primarily exists in organic forms, especially as sulfoxides and thiols/sulfides, which together account for approximately 78%.

3.3. FT-IR

The absorption peaks in the infrared spectrum of coal can be divided into the following four main types: (1) Absorption peaks located at $900\text{--}700\text{ cm}^{-1}$, corresponding to aromatic structures; (2) absorption peaks located at $800\text{--}1000\text{ cm}^{-1}$, associated with oxygen- and sulfur-containing heteroatom functional groups, stretching vibrations of aromatic ring C=C, and deformation vibrations of $-\text{CH}_3$ and $-\text{CH}_2$ groups; (3) absorption peaks located at $3000\text{--}2800\text{ cm}^{-1}$, representing aliphatic structures; and (4) absorption peaks located at $3600\text{--}3000\text{ cm}^{-1}$, corresponding to hydroxyl structures [19].

3.3.1. Hydroxyl Absorption Peaks

The hydroxyl groups in different types of coal exist as terminal groups and side chains, playing an essential role in the formation of hydrogen bonds in coal. To some extent, these groups determine the reactivity of coal. Hydroxyl groups exhibit strong activation effects during bond breaking and crosslinking. The absorption vibration wavenumber range of hydroxyl groups in FT-IR is $3600\text{--}3000\text{ cm}^{-1}$. The types of hydroxyl groups in the coal sample include OH-N hydrogen bonds, cyclic hydrogen bonds, OH-ether hydrogen bonds, OH-OH hydrogen bonds, and OH- π hydrogen bonds. As shown in Figure 4a, four peaks were fitted for the hydroxyl spectrum of the coal sample.

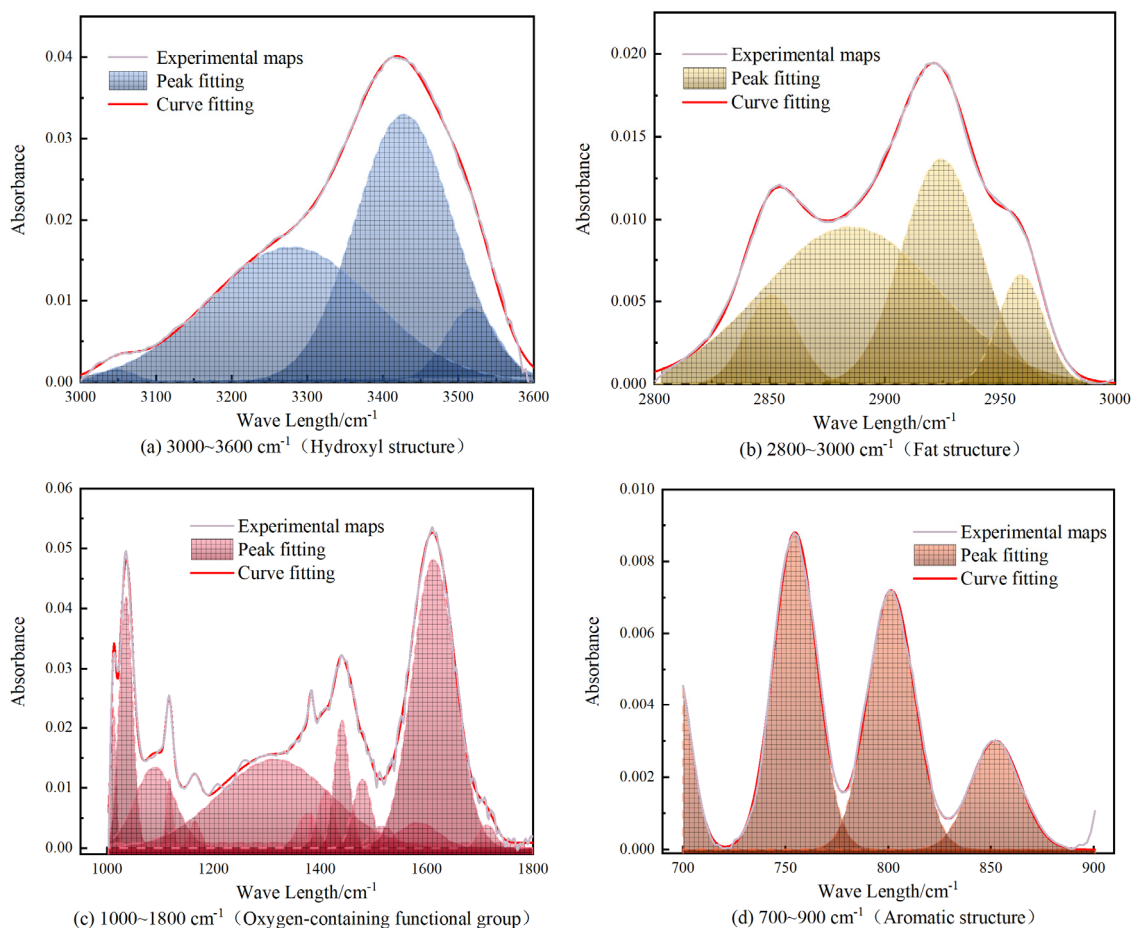


Figure 4. FT-IR Fitting Spectra.

The peak-fitting results of the hydroxyl spectrum of the coal sample indicate that there are four types of hydrogen bonds in coal. The OH-N hydrogen bonds (corresponding to $3002\text{--}3112\text{ cm}^{-1}$) account for 0.85% of the total hydroxyl groups, with a low content due to the presence of small amounts of nitrogen-containing aromatic compounds in the coal sample. The OH-O hydrogen bonds (corresponding to $3417\text{--}3600\text{ cm}^{-1}$) account for 7.39% of the total hydroxyl groups. The proportion of hydrogen bonds formed between hydroxyl groups and ether oxygen is relatively low, indicating limited direct interaction between ether oxygen groups (e.g., C-O-C) and hydroxyl groups in the sample. This type of structure has a certain impact on the polarity and water absorption properties of the sample. Hydrogen bonds formed between hydroxyl groups themselves, OH-OH hydrogen bonds (corresponding to $3206\text{--}3559\text{ cm}^{-1}$), account for 49.64%, enhancing intermolecular interactions and the chemical stability of the coal sample. The OH- π hydrogen bonds (corresponding to 3278 cm^{-1}) account for 42.10%, providing the sample with a certain

degree of stability and reactivity. It can be seen that self-associated hydrogen bonds between hydroxyl groups and OH- π hydrogen bonds are the dominant types (together accounting for 91.74%). This indicates that hydroxyl groups in the coal sample primarily interact with other hydroxyl groups and aromatic rings through intramolecular or intermolecular interactions, forming a complex intermolecular network.

3.3.2. Aliphatic Hydrocarbon Structures

Chain aliphatic hydrocarbons and cyclic aliphatic hydrocarbons are the primary forms of aliphatic hydrocarbon structures in coal. These structures correspond to the wavenumber range of 3000–2800 cm^{-1} in the FT-IR spectrum. As shown in Figure 4b, this range is deconvoluted into four peaks.

The peak-fitting results of the aliphatic hydrocarbon spectrum of the coal sample indicate that the functional group distribution shows the presence of a significant amount of methyl and methylene groups, corresponding to long-chain alkanes or similar structures. Methine groups (corresponding to 2885 cm^{-1}) account for 49.88% of the total area of aliphatic hydrocarbons and represent the primary functional group in the aliphatic hydrocarbons. Methylene groups (corresponding to 2850 and 2924 cm^{-1}) have a relative content of 40.99%. Methyl groups (corresponding to 2959 cm^{-1}) account for 9.14%. These findings indicate that the alkyl side chains in the gas coal sample are primarily composed of methylene and methine groups, with methyl groups as secondary components. This distribution suggests that the alkyl side chains in the coal sample predominantly consist of longer straight chains with fewer branches. Such a structure enhances molecular stability while increasing the yield of pyrolysis and volatile matter.

3.3.3. Oxygen-Containing Functional Groups

The oxygen-containing functional groups in coal primarily include hydroxyl groups ($-\text{OH}$), carboxyl groups ($-\text{COOH}$), carbonyl groups ($\text{C}=\text{O}$), and ether oxygen bonds ($\text{RO}-\text{R}'$). However, in the wavenumber range of 1800–1000 cm^{-1} , in addition to the presence of oxygen-containing functional groups, there are also absorption bands of aliphatic hydrocarbons and other features. The state of occurrence and distribution of these groups directly influence coal's adsorption and reaction properties. The fitting plot of oxygen-containing functional groups is shown in Figure 4c.

The peak-fitting results of the coal sample indicate that alkyl ethers ($\text{C}-\text{O}$, corresponding to approximately 1012 and 1035 cm^{-1}) account for 10.19%, suggesting the presence of a certain amount of aliphatic ethers in the coal sample, reflecting its relatively strong nonpolar components. Aryl ethers ($\text{C}-\text{O}-\text{C}$, corresponding to approximately 1089 and 1117 cm^{-1}) account for 9.33%, indicating the presence of aromatic rings connected by ether bonds in the coal sample, which enhances the chemical stability of the coal. Phenolic hydroxyls ($\text{C}-\text{O}$, corresponding to 1165–1314 cm^{-1}) account for 5.23% of the total area. Phenolic hydroxyl groups are minor functional sites in the coal sample, providing potential reactivity for oxidation or interaction with water molecules. The symmetric bending vibrations of $-\text{CH}_3$ (corresponding to 1346 and 1383 cm^{-1}) account for 27.44%, while the asymmetric bending vibrations of $-\text{CH}_3$ and scissoring vibrations of $-\text{CH}_2$ (corresponding to 1410 and 1460 cm^{-1}) account for 8.85% of the total area. This indicates that the alkyl structures in the coal sample are primarily composed of methyl groups, originating from short-chain hydrocarbons or branched hydrocarbons, which facilitate the release of volatile matter. Aromatic ring $\text{C}=\text{C}$ bonds (corresponding to 1479–1516 cm^{-1}) account for 4.49%, indicating that the coal sample contains relatively few aromatic components. However, as part of the molecular framework, they contribute to a certain degree of chemical stability. Conjugated carbonyl groups (corresponding to 1584 cm^{-1}) have a relative content of 2.65%.

Unsaturated carboxylic acid C=O bonds (corresponding to 1612 cm^{-1}) account for 31.49%. The high carboxyl content originates from the oxidation process of the coal and plays a key role in imparting hydrophilicity and reactivity, significantly influencing its combustion properties or chemical modification.

3.3.4. Aromatic Ring Structures

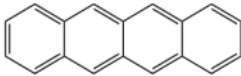
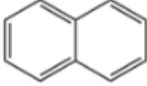
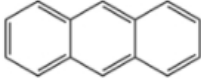
Aromatic rings are the primary structures in coal and the main carriers for gas adsorption. The study of aromatic structures in coal samples provides a theoretical foundation for the construction of coal molecular models and adsorption simulations. The wavenumber range of $900\text{--}700\text{ cm}^{-1}$ corresponds to the absorption vibration of aromatic hydrocarbon structures in coal. The substitution patterns of benzene rings determine the aromatic hydrocarbon structure. The peak fitting and optimized fitting spectrum of aromatic rings are shown in Figure 4d.

The fitting results indicate that there are three peaks in this range after second-order fitting. In the macromolecular structure of gas coal, benzene rings are primarily tri- and tetra-substituted (corresponding to 754 cm^{-1}) and di-substituted (corresponding to 801 cm^{-1}), with mono-substituted benzene rings (corresponding to 852 cm^{-1}) as secondary. In gas coal, the peak area of tri- and tetra-substituted benzene rings is 0.23, with a relative area proportion of 46.01%, indicating a significant presence of polysubstituted aromatic compounds. These structures are typically formed during coal pyrolysis through free radical reactions or aromatic ring cyclization. The substitution positions on the benzene ring influence the stability and chemical properties of the molecule, and tri- and tetra-substituted aromatic structures are generally more stable and occupy a larger proportion in gas coal. The peak area of di-substituted benzene rings is 0.20, with a relative area proportion of 36.65%, further indicating a high level of substitution complexity in the aromatic rings of gas coal. The peak area of mono-substituted benzene rings is 0.09, with a relative area proportion of 16.39%, indicating that single benzene ring structures are relatively scarce in the molecular structure of gas coal. This suggests that the macromolecular structure of gas coal contains more aromatic compounds forming complex network structures, with multiple substituents interacting with each other.

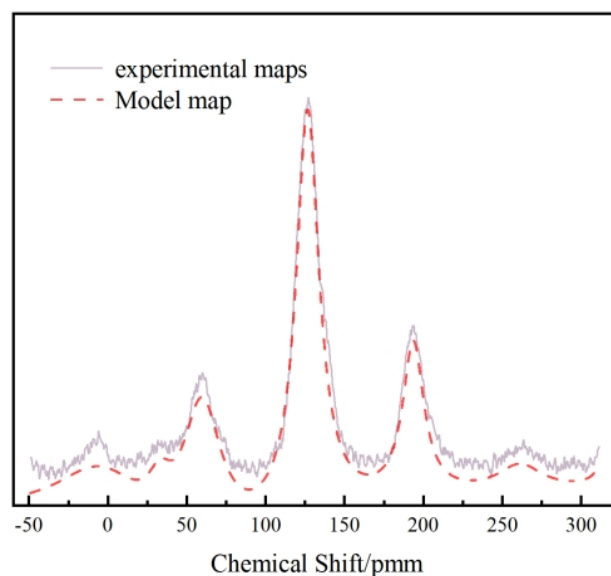
3.4. Construction and Validation of the Coal Molecular Plane Model

The bridge carbon to peripheral carbon ratio of the coal sample is 0.28, indicating that its aromatic structures primarily exist in the forms of benzene and naphthalene. By adjusting the number of aromatic condensed rings, the aromatic structure distribution that best matches the coal sample's bridge-to-peripheral ratio is determined, as shown in Table 4. Based on the data in the table, the number of aromatic carbons in the coal sample is calculated to be 100. Combined with ^{13}C -NMR analysis, the aromatic carbon ratio of gas coal is 49.32%, yielding a total macromolecular carbon count of 204 for the coal sample. According to elemental analysis, the mass fractions of carbon, oxygen, nitrogen, and sulfur in the coal are 85.11%, 9.36%, 0.78%, and 0.73%, respectively, corresponding to 17 oxygen atoms, 1 nitrogen atom, and 1 sulfur atom. According to XPS analysis, nitrogen in the coal sample primarily exists in the form of pyrrolic nitrogen ($\text{C}_4\text{H}_5\text{N}$), while sulfur mainly exists as sulfoxides and sulfones. However, sulfoxides, sulfones, thiols, and sulfides tend to detach during the coalification process. Therefore, sulfur is considered primarily in the form of thiophenic sulfur ($\text{C}_4\text{H}_4\text{S}$). This indicates that the molecular structure of the coal sample includes one pyrrolic nitrogen atom and one thiophenic sulfur atom.

Table 4. Forms of Aromatic Structures in the Coal Macromolecular Configuration.

Type	Quantity/Count	Type	Quantity/Count
	3		1
	6		1
	5		1

The planar structural model of gas coal was drawn using KingDraw v5.0, and the data were imported into MestReNova-15.0.0-34764 software to generate the calculated ^{13}C -NMR spectrum of the model. Subsequently, the calculated ^{13}C -NMR spectrum of the model was compared with the experimental ^{13}C -NMR spectrum using Origin 2018. The structural model was refined by adjusting the connections of various structural units in the model. Finally, the comparison between the calculated ^{13}C -NMR spectrum of the coal sample model and the experimental ^{13}C -NMR spectrum is shown in Figure 5. Figure 6 shows the planar molecular structure of gas coal, with the molecular formula $\text{C}_{204}\text{H}_{117}\text{O}_{17}\text{NS}$. A comparison of the elemental analysis results between the model and the actual coal sample is presented in Table 5.

**Figure 5.** Comparison of Experimental ^{13}C NMR Spectrum and Model-Calculated Spectrum of the Coal Sample.**Table 5.** Comparison of Elemental Content Between Actual Coal Sample and Molecular Model.

Coal Sample	$\text{N}_{\text{daf}}/\%$	$\text{C}_{\text{daf}}/\%$	$\text{H}_{\text{daf}}/\%$	$\text{S}_{\text{daf}}/\%$	$\text{O}_{\text{daf}}/\%$
Measured	0.78	85.11	4.02	0.73	9.36
Model	0.49	84.89	4.09	1.11	9.42
Error	0.29	0.22	0.07	0.38	0.06

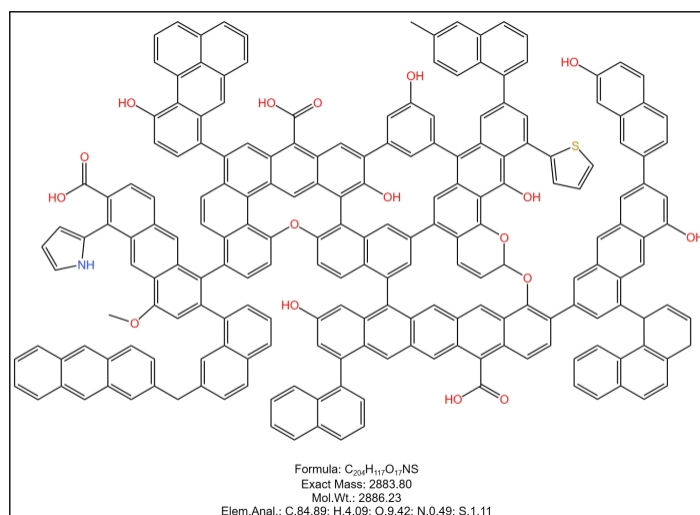


Figure 6. Planar Structure of the Coal Macromolecule.

3.5. Optimization and Analysis of Coal Molecular Structure Model

3.5.1. Energy Optimization

The 2D planar molecular model of gas coal was imported into the Materials Studio software, where hydrogen saturation was applied to generate the initial 3D structure, as shown in Figure 7a. The Forcite module was used to perform geometry optimization, annealing treatment, and dynamic simulation on the model. The COMPASS II force field was employed, with the calculation precision set to Medium, and charge values were automatically assigned to enhance simulation consistency [20,21]. Dynamic simulations were carried out over five cycles within a temperature range of 300 K to 600 K to account for the effect of thermal motion on the structure. The annealing process involved heating and cooling cycles to drive the molecular system toward a global minimum energy state [22,23]. Finally, as shown in Figure 7b, a low-energy macromolecular structure of gas coal was obtained after multiple rounds of optimization and processing.

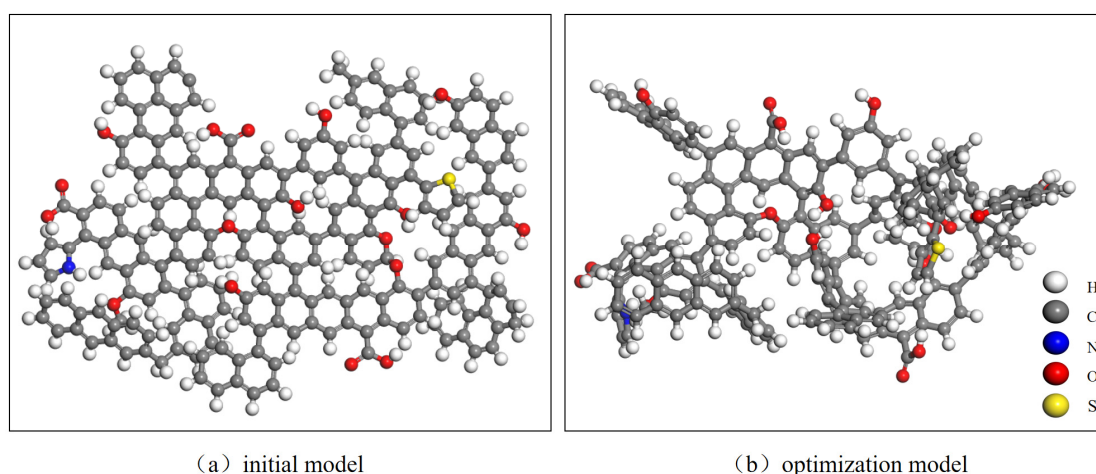


Figure 7. Comparison of the Model Before and After Optimization.

As shown in Table 6, the energy changes in the gas coal macromolecular structure model are significant before and after optimization. In its initial state, the total valence electron energy is $6113.94 \text{ kcal}\cdot\text{mol}^{-1}$, indicating a high level of chemical bond tension, with the molecular model yet to reach its lowest energy state. After geometric optimization, the valence electron energy significantly decreased; bond stretching energy was reduced to $66.04 \text{ kcal}\cdot\text{mol}^{-1}$, and bond angle energy decreased to $158.32 \text{ kcal}\cdot\text{mol}^{-1}$, indicating a

substantial reduction in internal stress within chemical bonds. Torsional energy slightly increased to $3914.58 \text{ kcal}\cdot\text{mol}^{-1}$, which remained the primary component of valence electron energy. This suggests that the spatial configuration stability of the coal molecule is primarily dependent on the bending and torsion of chemical bonds. The inversion energy increased to $24.19 \text{ kcal}\cdot\text{mol}^{-1}$, indicating that the optimized stereostructure underwent some adjustments.

Table 6. Energy Changes Before and After Model Optimization.

State	Bond Energy/ $\text{kcal}\cdot\text{mol}^{-1}$	Angle Energy/ $\text{kcal}\cdot\text{mol}^{-1}$	Torsion Energy/ $\text{kcal}\cdot\text{mol}^{-1}$	Inversion Energy/ $\text{kcal}\cdot\text{mol}^{-1}$	Van der Waals Energy/ $\text{kcal}\cdot\text{mol}^{-1}$	Electrostatic Energy/ $\text{kcal}\cdot\text{mol}^{-1}$	Total Energy/ $\text{kcal}\cdot\text{mol}^{-1}$
Initial	1912.78	391.89	3806.98	2.29	996.31	-132.15	8525.12
Final	66.04	158.32	3914.58	24.19	164.56	-251.31	3966.16

The non-bond energy consists of van der Waals energy and electrostatic energy. In the initial state, the van der Waals energy is $996.31 \text{ kcal}\cdot\text{mol}^{-1}$, which accounts for the major portion of the non-bond energy, while the electrostatic energy is $-132.15 \text{ kcal}\cdot\text{mol}^{-1}$, resulting in a total non-bond energy of $864.16 \text{ kcal}\cdot\text{mol}^{-1}$. After optimization, the van der Waals energy significantly decreased to $164.56 \text{ kcal}\cdot\text{mol}^{-1}$, while the electrostatic energy dropped to $-251.31 \text{ kcal}\cdot\text{mol}^{-1}$, resulting in a final total non-bond energy of $-86.75 \text{ kcal}\cdot\text{mol}^{-1}$. This represents a reduction of $950.91 \text{ kcal}\cdot\text{mol}^{-1}$ compared to the initial state, indicating that intermolecular weak interactions were significantly optimized, molecular packing became more compact, and electrostatic attraction was enhanced.

The final optimized model's total valence electron energy decreased to $4163.13 \text{ kcal}\cdot\text{mol}^{-1}$, a reduction of $1950.81 \text{ kcal}\cdot\text{mol}^{-1}$ compared to the initial state, indicating a significant improvement in the overall stability of the model. The optimization results show that the stability of the coal molecule primarily depends on the contribution of valence electron energy, with bond torsional energy playing a dominant role and being critical to the stability of the spatial configuration. Additionally, the van der Waals forces in the non-bond energy significantly contribute to the optimization of intermolecular weak interactions. Overall, the optimized coal molecular model achieved a more stable and three-dimensional structure through adjustments in bond bending, torsion, and intermolecular interactions.

3.5.2. Surface Electrostatic Potential (ESP) Distribution

The ESP distribution characteristics on the surface of the coal molecule were calculated using the DMol3 module in the MS 2020 software. The ESP projection on the van der Waals surface was obtained through charge density analysis. The results show that red areas represent positive ESP values, while blue areas indicate negative ESP values. The intensity of the color reflects the magnitude of the absolute ESP value. The simulation results are shown in Figure 8.

The maximum electrostatic potential (ESP) value on the surface of the gas coal molecule is 0.1006 a.u. , while the minimum ESP value is -0.09730 a.u. Locations with smaller negative ESP values are more prone to electrophilic reactions, while regions with larger positive ESP values tend to undergo nucleophilic reactions. The maximum ESP value corresponds to functional groups in the positively charged regions of the surface, specifically hydrogen bond acceptor areas, while the minimum ESP value is associated with oxygen atoms in oxygen-containing functional groups. The difference between the maximum and minimum ESP values is approximately 0.1979 a.u. , indicating a highly heterogeneous charge distribution on the surface of the gas coal molecule. This heterogeneity reveals the presence of

distinct polar regions on the gas coal surface, which can interact differently with polar and nonpolar molecules.

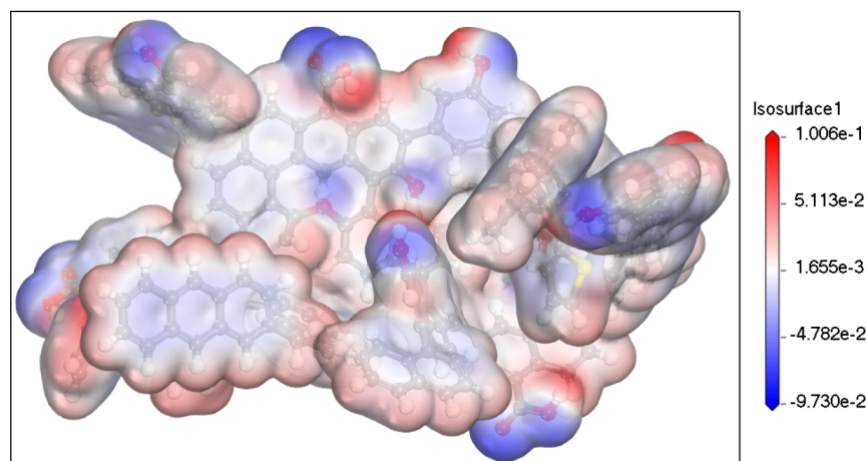


Figure 8. Electrostatic Potential Distribution of the Gas Coal Molecule.

4. Conclusions

- (1) Gas coal is characterized by high carbon content (85.11%), low sulfur content (0.73%), and moderate oxygen content (9.36%). Aromatic carbon accounts for 49.32% of the total carbon, mainly in the form of benzene and condensed ring structures. Nitrogen exists primarily as pyrrolic nitrogen (65.54%), while sulfur is mainly present as sulfoxides (50.55%) and sulfides (27.60%). Hydroxyl groups are dominated by self-associated hydrogen bonds (49.64%) and OH- π hydrogen bonds (42.10%). Among oxygen-containing functional groups, carboxyl groups (31.49%) and carbonyl groups significantly enhance the sample's polarity and reactivity.
- (2) Based on the characterization and analysis data, a molecular model of gas coal ($C_{204}H_{117}O_{17}NS$) was constructed and validated through simulation. The discrepancy between the experimental and model elemental compositions is less than 1%, accurately reflecting the molecular structural characteristics of gas coal.
- (3) Through molecular mechanics and annealing dynamics optimization, the total molecular energy was reduced from $8525.12 \text{ kcal}\cdot\text{mol}^{-1}$ to $3966.16 \text{ kcal}\cdot\text{mol}^{-1}$. The van der Waals energy and electrostatic energy were significantly optimized, resulting in tighter molecular packing and greatly enhanced stability. Torsional energy in valence electron energy dominates the spatial configuration of the molecule, while van der Waals forces and electrostatic attraction in non-bond energy are key factors in optimizing intermolecular weak interactions.
- (4) Using the constructed molecular structure model, further research will be conducted on the combustion and gasification mechanisms of gas coal from the Ningxia Hong II coal mine. This will provide theoretical guidance for the efficient development and utilization of coal resources, as well as pollutant emission control, thereby offering technical support for the clean and efficient use of coal.

Author Contributions: Conceptualization, Methodology, Writing—Original Draft Preparation, X.C.; Funding Acquisition, Supervision, L.H.; Writing—Review and Editing, Investigation, Visualization, D.Z. and D.G. All authors have read and agreed to the published version of the manuscript.

Funding: This research was funded by the National Natural Science Foundation of China (No. 51004062).

Data Availability Statement: The original contributions presented in this study are included in the article. Further inquiries can be directed to the corresponding author.

Conflicts of Interest: The authors declare no conflicts of interest.

References

1. Li, Q.; Li, Q.; Han, Y. A Numerical Investigation on Kick Control with the Displacement Kill Method during a Well Test in a Deep-Water Gas Reservoir: A Case Study. *Processes* **2024**, *12*, 2090. [\[CrossRef\]](#)
2. Li, Q.; Li, Q.; Wang, F.; Wu, J.; Wang, Y. The Carrying Behavior of Water-Based Fracturing Fluid in Shale Reservoir Fractures and Molecular Dynamics of Sand-Carrying Mechanism. *Processes* **2024**, *12*, 2051. [\[CrossRef\]](#)
3. Wang, C.; Xing, Y.; Shi, K. Chemical Structure Characteristics and Model Construction of Coal with Three Kinds of Coalification Degrees. *ACS Omega* **2024**, *9*, 1881–1893. [\[CrossRef\]](#)
4. Mathews, P.J.; Chaffee, L.A. The molecular representations of coal—A review. *Fuel* **2012**, *96*, 1–14. [\[CrossRef\]](#)
5. Jiang, Y.; Yang, X.; Ma, H. Modelling the Mechanism of Sulphur Evolution in the Coal Combustion Process: The Effect of Sulphur–Nitrogen Interactions and Excess Air Coefficients. *Processes* **2023**, *11*, 1518. [\[CrossRef\]](#)
6. Zhang, H.; Xian, S.; Zhu, Z. Release behaviors of sulfur-containing pollutants during combustion and gasification of coals by TG-MS. *J. Therm. Anal. Calorim.* **2020**, *143*, 377–386. [\[CrossRef\]](#)
7. Wang, J.; Zhao, X. Key technologies and demonstration of clean and efficient cascade utilization of low rank coal. *J. Chin. Acad. Sci.* **2012**, *27*, 382–388.
8. Sharma, A.; Kyotani, T.; Tomita, A. A new quantitative approach for microstructural analysis of coal char using HRTEM images. *Fuel* **1999**, *78*, 1203–1212. [\[CrossRef\]](#)
9. Xiang, J.; Zeng, F.; Liang, H. Model construction of the macromolecular structure of Yanzhou Coal and its molecular simulation. *J. Fuel Chem. Technol.* **2011**, *39*, 481–488. [\[CrossRef\]](#)
10. Li, Z.; Wang, Y.; Li, P. The macromolecular model construction and quantum chemical calculation of Hongshiwan coal in Ningdong. *J. Chem. Eng.* **2018**, *69*, 2208–2216. (In Chinese)
11. Zhang, D.; Li, Y.; Chang, L. Structural characteristics and molecular model construction of Mile lignite. *J. Fuel Chem.* **2021**, *49*, 727–734. (In Chinese)
12. Fan, Z. *Study on Macromolecular Modeling and Adsorption Mechanism of Different Rank Coal*; China University of Geosciences: Beijing, China, 2020.
13. Ben, Z.; Xian, D.; Yu, F. Structural Characterization and Molecular Model Construction of High-Ash Coal from Northern China. *Molecules* **2023**, *28*, 5593. [\[CrossRef\]](#) [\[PubMed\]](#)
14. GB/T482-2008; Method for Taking Coal Seam Samples. China Standard Press: Beijing, China, 2008.
15. GB/T212-2008; Proximate Analysis of Coal. China Standard Press: Beijing, China, 2008.
16. GB/T31391-2015; Ultimate Analysis of Coal. China Standard Press: Beijing, China, 2015.
17. Lina, Q.; Long, L.; Jin, C. Molecular Model Construction and Optimization Study of Gas Coal in the Huainan Mining Area. *Processes* **2022**, *11*, 73. [\[CrossRef\]](#)
18. Shi, Y.; Zhu, Y.; Chen, S. Structural Characterization and Molecular Model Construction of Lignite: A Case of Xianfeng Coal. *Energies* **2024**, *17*, 1049. [\[CrossRef\]](#)
19. Jin, J.; Yu, W.; Dan, Z. Molecular structure characterization analysis and molecular model construction of anthracite. *PLoS ONE* **2022**, *17*, e0275108.
20. Chao, X.; Wen, W.; Kai, W. Filling–adsorption mechanism and diffusive transport characteristics of N₂/CO₂ in coal: Experiment and molecular simulation. *Energy* **2023**, *282*, 128428.
21. Zhang, J.; Clennell, B.M.; Liu, K. Molecular dynamics study of CO₂ sorption and transport properties in coal. *Fuel* **2016**, *177*, 53–17762. [\[CrossRef\]](#)
22. Feng, W.; Li, Z.; Gao, H.; Wang, Q.; Bai, H.; Li, P. Understanding the molecular structure of HSW coal at atomic level: A comprehensive characterization from combined experimental and computational study. *Green Energy Environ.* **2021**, *6*, 150–159. [\[CrossRef\]](#)
23. Liu, H.; Jiang, B.; Song, Y.; Hou, C. The tectonic stress-driving alteration and evolution of chemical structure for low- to medium-rank coals—by molecular simulation method. *Arab. J. Geosci.* **2019**, *12*, 726. [\[CrossRef\]](#)

Disclaimer/Publisher’s Note: The statements, opinions and data contained in all publications are solely those of the individual author(s) and contributor(s) and not of MDPI and/or the editor(s). MDPI and/or the editor(s) disclaim responsibility for any injury to people or property resulting from any ideas, methods, instructions or products referred to in the content.